

Electric conductivity percolation in naturally dehydrating, lightly wetted, hydrophilic fumed silica powder

Dagmara Sokolowska, Daniel Dziob, Urszula Gorska, Bartosz Kieltyka, and Jozef K. Moscicki*

Smoluchowski Institute of Physics, Jagiellonian University, Reymonta 4, 30-059 Krakow, Poland

(Received 25 January 2012; revised manuscript received 23 November 2012; published 7 June 2013)

In studying the dehydration of surface-moistened fumed silica Aerosil powders, we found a conductivity percolation transition at low hydration levels. Both the percolation exponent and the threshold are typical for correlated site-bond transitions in complex two-dimensional (2D) systems. The exponent values, 0.94–1.10, are indicative of severe heterogeneity in the conducting medium. The surface moisture at the percolation threshold takes on a universal value of $0.65 \text{ mg}_{\text{[H}_2\text{O]}}/\text{m}^2_{\text{[silica]}}$, independent of the silica grain size, and equivalent to twice the first hydration monolayer. This level is just sufficient to sustain a quasi-2D, hydrogen-bonded water network spanning the silica surface.

DOI: [10.1103/PhysRevE.87.062404](https://doi.org/10.1103/PhysRevE.87.062404)

PACS number(s): 68.08.Bc, 64.60.ah, 47.55.nd, 66.10.Ed

I. INTRODUCTION

Conductivity percolation in a heterogeneous conductor-insulator system is observed and parametrized in terms of the percolation exponent and the threshold composition. At the peak period of fascination with phase transitions, intensive studies were performed on theoretical and experimental models of the percolation phenomenon. These studies concentrated, on the one hand, on the relation between the exponent and the threshold, and on the other hand, on the medium dimensionality, the percolation mechanism (bond and site), and the medium character and details (network or continuum, periodical or random, etc.) [1].

The result that bears direct consequences for studying heterogeneous systems is the discriminating dependence of the exponent on the medium dimensionality. This has already been exploited, e.g., in electric conductivity studies *in vitro* of simple biological systems of various complexity: maize seeds [2,3], biological membranes [4], crustacean embryos [5], and protein powders [6–9], as well as *in vivo* in living lichens [10,11], yeast [12], and blue-green algae [13]. The conducting media are the hydrogen-bonded networks of water molecules, and conductivity is protonic in nature [8,14,15].

In the course of dehydration, one or two separate percolation transitions were observed in these systems. The first transition was observed in the diminishing three-dimensional water continuum at high water content. The second transition was observed at much lower water content, when the hydration water disappears from the biosystem's water-accessible surface. The low hydration percolation transition is especially attractive and promising for biological studies because this transition usually occurs at water contents typical for onset of physiological activities in biosystems [3,6,16–18]. These findings provoked extensive numerical modeling studies by Brovchenko, Oleinikova, and colleagues [17–27]. Considering the organization of water molecules on different surfaces with increasing levels of biomimicry, they found that the percolating, hydrogen-bonded water network at the surface is indeed two dimensional (2D) in character and that percolation is mixed bond-site in nature.

In the vicinity of the low hydration percolation threshold, conductivity depends on the probability that electric charge carriers will find unrestricted passage in the studied medium. It is commonly assumed that this probability is directly proportional to the degree of hydration, which can be parametrized, e.g., by the ratio of the water mass in the sample to the dry sample mass (“dry mass”), h ; or, if the specific surfaces, S , are known, by the water mass per specific surface (hereafter referred to as the surface moisture), $\rho = h/S$:

$$(\sigma - \sigma^*) \propto (h - h^*)^\mu \propto (\rho - \rho^*)^\mu, \quad \text{for } h > h^* \text{ and } \rho > \rho^*, \quad (1)$$

with μ being the percolation exponent, and the asterisk denoting residual (background) values for conductivity, hydration, or surface moisture at the percolation threshold. For the uncorrelated and uniform percolation on the idealized 2D conductor-insulator infinite lattice, μ takes the universal value of $\mu_o = 1.299$ [28–30], while values of h^* and σ^* depend on the lattice structure and the failure mechanism. Careri and colleagues demonstrated that the observed low hydration conductivity in biological systems is due to the motion of protons along the network of hydration water “threads” [2,4–6,14]. They also found that the conduction takes place in localized patches of water on the surface rather than across the whole sample.

Water-accessible surfaces (free surface area) of biomaterials are anything but Euclidean, 2D systems, and their mechanical and chemical properties are highly heterogeneous. Thus, not only the structure of the water layer but also the degradation of the conducting network during dehydration is inhomogeneous on these surfaces. As a result, conductivity percolation with a nonuniversal exponent, $\mu = 1.08$ – 1.46 , is observed in these systems [4–8,10–13]. Despite the span, most of the values fall in the range seen when modeling conductivity percolation phenomena in 2D, both experimentally and theoretically. The hydration threshold, in turn, is generally noninformative about water organization at the surface because it compares water mass at the threshold to dry material mass rather than to the specific surface area and morphology of the surface. Not surprisingly, the threshold values have been found to vary widely over orders of magnitude from system to system

*jozef.moscicki@uj.edu.pl

(see Table I in [13]), and quantitative interpretation has been difficult [6,11,19].

To better understand water organization at the surface of biological and biosimilar systems—or to at least shed some more light on details of the observed hydration water film percolation—we have continued experimental efforts, this time with conductivity at the wet surface of hydrophilic Aerosil. The material consists of nonconducting, molten grains of silicon dioxide, which are coated with hydrophilic silanol groups that facilitate, via hydrogen bonding, formation of the hydrogen-bonded water network film on the surface [31]. Importantly, proton conduction was observed in the system and the mechanism of this conduction does not depend on the amount of water present [32,33]. The advantage of studying silica powders is in the consistency of their primary particles' shapes, and in the ability to control the particles' dimensions and specific surface area [34,35]. Controllability of surface hydrophilic and hydrophobic properties in principle allows the research environment to mimic properties of specific surfaces of different biological systems, e.g., globular proteins or yeast cells [31]. We hoped that such control would make it possible to “calibrate,” e.g., the conductivity percolation parameters against the geometrical and chemical parameters of the silica surface. Additionally, the powders are controllable model systems for comparing experimental results with predictions of numerical simulations [17–27]. This way we should be able, in the future, to better glimpse water's secret “social life” on biological and similar surfaces.

II. MATERIALS AND METHODS

Evonik Industries generously provided three hydrophilic Aerosil powders for this study. The manufacturer characterizes these powders by the mean specific surface area S : (A90) $90 \pm 15 \text{ m}^2/\text{g}$, (A150) $150 \pm 15 \text{ m}^2/\text{g}$, and (A380) $380 \pm 30 \text{ m}^2/\text{g}$, and by surface density of silanol groups $2.5 \text{ SiOH}/\text{nm}^2$ [34]. Because the complete high temperature dehydration dehydroxylates the Aerosil surface, leaving behind the siloxane bonds—which are hydrophobic and thus probably serve as poor hydration sites in the reverse process [36]—we used the factory-dry powders as provided. Spontaneous gelation of fumed silica at higher water contents makes control of silica powder hydration a tedious, elaborate, and very time-consuming task. We succeeded by trial and error to find a proper hydration routine that repeatedly produced just surface-wet samples of Aerosil powders, far below the gelation threshold. The powder was exposed to a very fine mist of fresh water produced by an ultrasonic humidifier (Boveco 7131) for a period of 5–6 h, isopiastically at ambient atmospheric pressure, and with mist temperatures just below 40°C . Initial water intake by a sample was notably very slow, about $0.15 \text{ g}_{[\text{H}_2\text{O}]}/\text{g}_{[\text{silica}]}$ in total, during a period of 4–5 h. At some point near the end of that period, the hydration process picked up speed and the sample gained on the order of $0.85 \text{ g}_{[\text{H}_2\text{O}]}/\text{g}_{[\text{silica}]}$ in the next 30–45 min. This rapid intake was allowed to continue long enough (as determined by trial and error) to moisten the primary particles' surface, but was halted soon enough to avoid gelation [35]. Several batches of wet Aerosil powder were prepared this way, with the cutoff

instance selected arbitrarily by visually following the sample opacity.

The moistened material was immediately transferred into a custom-made parallel plate capacitor cell [12,13]. The cell was connected to the HP 4192A LF impedance analyzer by two pairs of loosely coiled, thin wires (four-point method), and the complex dielectric permittivity, $\varepsilon^*(\nu) = \varepsilon'(\nu) - i\varepsilon''(\nu)$, was sampled at a number of discrete frequencies between $\nu = 10 \text{ Hz}$ and 10 MHz .

Water content in the sample was monitored continuously to within $20 \mu\text{g}$ accuracy with a laboratory microbalance (Radwag-WPS72). Desiccation of each sample proceeded via still air at a natural evaporation rate, usually $0.05\text{--}0.15 \text{ g}/\text{h}$, at the ambient air temperature of $T = 23^\circ\text{C}\text{--}25^\circ\text{C}$. Dielectric spectra and cell weight were recorded every 180 s during the process.

III. RESULTS

The conductivity data presented in detail are of samples with an initial surface moisture of 27.0 (A90), 9.4 (A150), and $10.8 \text{ mg}_{[\text{H}_2\text{O}]}/\text{m}^2_{[\text{silica}]}$ (A380). The results are representative for all batches studied. Typical spectra of dielectric permittivity, $\varepsilon'(\nu)$, and of the dielectric loss factor, $\varepsilon''(\nu)$, are shown in Fig. 1. It is generally accepted that such patterns are due to the presence of hopping charge carriers, accumulation of charges, and charge and discharge currents. The patterns are in agreement with the expected proton-hopping nature of the conductivity of wet sands, porous silica, and biological systems [2,4,5,31,37–43].

At the low-frequency end, the dielectric loss factor is dominated by the static conductivity, σ , manifested by a nearly $\varepsilon''(\nu) \propto \nu^{-1}$ dependence. In fact, at low hydration levels, all spectra in this frequency range follow Jonscher's “universal dielectric response” [44],

$$\varepsilon^*(\nu) = B_1 \nu^{n_1-1} - i B_2 \nu^{n_2-1}, \quad (2)$$

with n_1 and n_2 close to zero, the latter being indicative of the absence of the electrode polarization effect in the spectra. This allowed us a straightforward extraction of σ from the dielectric loss spectrum by fitting the low-frequency linear portion of the

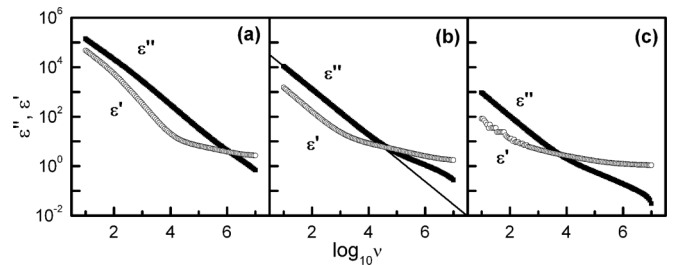


FIG. 1. Lightly moistened, hydrophilic Aerosil powders freely desiccating to ambient air; typical evolution of dielectric permittivity, ε' (open circles), and dielectric loss, ε'' (filled circles) spectra shown for the A150 sample at three different water surface loads: (a) $h = 1.417$, (b) $h = 0.727$, and (c) $h = 0.152 \text{ (g}_{[\text{H}_2\text{O}]}/\text{g}_{[\text{silica}]})$; the straight line in (b) demonstrates the conductivity contribution.

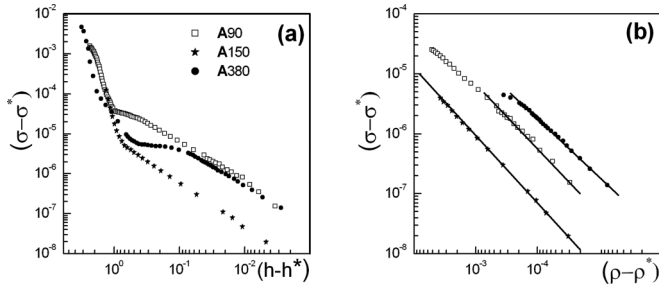


FIG. 2. Lightly moistened, hydrophilic Aerosil powders freely desiccating to ambient air. Double-logarithmic plots of conductivity σ (S/m) (a) vs hydration level, h ($\text{g}_{[\text{H}_2\text{O}]}/\text{g}_{[\text{silica}]}$), in the whole hydration range studied, and (b) vs surface moisture, ρ ($\text{g}_{[\text{H}_2\text{O}]}/\text{m}^2_{[\text{silica}]}$), in the proximity of the percolation transition at low-hydration levels. To emphasize presence of the transition, the quantities are plotted relative to values at the percolation threshold (denoted by the asterisk; see Table I.). Straight solid lines are the linear regression fits to data.

dielectric loss spectrum component with

$$\log[\varepsilon''(\nu)] = \log[\sigma(h)/\varepsilon_0] - (n_2 - 1)\log(2\pi\nu), \quad (3)$$

with ε_0 being the permittivity of the vacuum.

Typical results of conductivity vs hydration are shown in Fig. 2(a). With percolation parameters generally unknown, and thus treated as fittable parameters, we proceeded as follows. After choosing graphically reasonable starting values for ρ^* and σ^* , we used linear regression to analyze the conductivity data in the log-log representation. Repeating the procedure while sweeping appropriate ranges of ρ^* and σ^* until the best chi square was found yielded the set of critical parameters. The procedure turned out to be very sensitive to ρ^* and σ^* , and rapidly converging. Final results are shown in Fig. 2(b), and the fit parameters are summarized in Table I.

It should be emphasized that, regardless of the size of the primary Aerosil particles, continuous dehydration of every sample studied led to the same value of nonzero conductivity of the “equilibrium dry mass” of $\sigma_o = 1.010^{-8}$ S/m, which remained unchanged even after 3 days of the samples’ continued exposure to air.

TABLE I. Samples characteristics and conductivity percolation parameters; h^* and ρ^* are percolation hydration and surface moisture thresholds, respectively, and μ is the scaling exponent.

Sample	Aerosil A90	Aerosil A150	Aerosil A380
Specific surface area, S (m^2/g)	$90_{\pm 15}$	$150_{\pm 15}$	$380_{\pm 30}$
Primary particle mean size, d (nm)	20	14	7
Sample dry mass (g)	$1.06_{\pm 0.01}$	$0.73_{\pm 0.01}$	$0.64_{\pm 0.01}$
h^* ($\text{g}_{[\text{H}_2\text{O}]}/\text{g}_{[\text{silica}]}$)	$0.057_{\pm 0.003}$	$0.098_{\pm 0.005}$	$0.244_{\pm 0.003}$
$\rho^* = h^*/S$ ($\text{mg}_{[\text{H}_2\text{O}]}/\text{m}^2_{[\text{silica}]}$)	$0.64_{\pm 0.14}$	$0.65_{\pm 0.10}$	$0.64_{\pm 0.06}$
μ	$0.94_{\pm 0.02}$	$1.10_{\pm 0.01}$	$1.01_{\pm 0.01}$

IV. DISCUSSION

The observed percolation parameters are derivatives of static and dynamic properties of the hydrogen-bonded water network [31,45]. The first and most obvious observation emerging from our results is (see Table I) that the percolation exponent, μ , and the threshold surface moisture, ρ^* , do not vary significantly with the primary particle size. Thus, surface mechanical and chemical structures are invariant, universal properties of the Aerosil material [46].

The percolation exponent values are close to the 1.08 value observed for yeast colonies [12]; we anticipated such similarity. Because the mechanical and chemical topology of the specific surface of pyrogenic silica is quite complicated, a number of different uncorrelated mechanisms can lead to the percolation exponent close to unity. One possible mechanism is that the hydrophilicity of the surface is not uniform; the surface is populated with intermingled patches of highly hydrophilic silanol groups and hydrophobic siloxane groups as reflected in relatively low mean surface density of silanol groups at the Aerosil surface (about $2.5 \text{ SiOH}/\text{nm}^2$ [34]). Even within the hydrophilic areas, surface density of silanol groups varies substantially. As a result, experimental observation showed different structural systems of water bound at the surfaces: high-density, weakly associated, small clusters with strongly distorted hydrogen bonds; strongly associated nano- and microdomains of “icelike” water; and a continuous layer with both [47,48]. One of the conductivity percolation pathways would then be via the water layer failure—its progressive perforation during dehydration—that is observed even at flat mica surfaces [49]. During critical dehydration, the water layer inevitably breaks down into a network of channels, ponds, and isolated reservoirs. Thus the current permeability would depend on the “dry-land” pattern—the distribution of water channels, resistance variations, and relative fluctuations due to variation in sizes of the channels and ponds—in a manner analogous to that considered in the conductivity percolation model of Halperin *et al.* [50]. Halperin *et al.* estimated the percolation parameters in a continuous “Swiss-cheese” 2D system: a homogeneous, conducting, 2D film punctured randomly with round holes, resulting in a “nodes-links-blobs” conducting medium. They found the lower-bound estimate of approximately 1 for the critical exponent, and this prediction was subsequently verified experimentally ($\mu \approx 1.1$ [51]).

Another possible pathway affecting the percolation exponent is the disappearance of the proton-wires network in the presence of a nonzero residual “background” conductivity of 1.0×10^{-8} S/m, which we observed repeatedly in dry-to-air Aerosil samples. This level of conductivity is comparable to the conductivity of ice [52]. This similarity might be indicative of the background conduction process taking place in strongly bound, icelike water patches. These icelike patches are difficult to remove without heating the silica to extremely high temperatures, they are known to exist in biological systems [11], and they also show up in computer simulations of water at protein surfaces [19]. Straley proposed a model that accounts for the percolation in just such a situation [53]. He considered systems of random resistor lattices, in which the lattice element can switch between two different nonzero

resistance values rather than only between the limiting isolator and conductor states. As a result, he obtained exponent values of 1.10 for the bond percolation and 1.25 for the site percolation for the 2D lattice.

Finally, we cannot completely ignore the geometric constraints of the measurement. The alternating current technique commonly used to follow conductivity percolation probes local rather than spatially unlimited proton migration, as already emphasized to explain conductivity percolation in purple membrane [4]. This situation was modeled by Berkowitz and Knight, who considered conductivity percolation in a 2D medium limited in the size and found that the limitation also leads to lowering of the exponent value to $\mu \approx 1$ [54].

The complex picture of the percolation transition is also consistent with the outcomes of extensive numerical studies, which have shown that the model water network percolation on idealized hydrophilic surfaces, either flat or curved, is random bond-site and quasi-2D in nature [20,23,24]. In conjunction with this finding we note that, in response to the mechanical and chemical heterogeneity of natural Aerosil surfaces, the spatial geometry of the hydrogen-bonded network at the surface and the randomness of the network decomposition mechanism could vary from system to system. As a result, in some cases—even on the same surface, but with different hydration or dehydration history—the spatial geometry can be more “bond” than “site” or vice versa, with the exponent taking on different values, e.g., between 1.1 (bond) and 1.25 (site) if we follow Straley’s prediction [53]. This would explain the variation in scaling exponent values for Aerosil powders and for most of the biological systems studied, from 1.08 for yeast [12], through 1.18 for lichen *C. mitis* [10], and 1.23 for maize seeds and purple membrane [2,4].

We found the same surface moisture at the percolation threshold for all different Aerosil primary particle sizes studied (see Table I). The amount of water at the threshold is, however, quite substantial. Assuming full hydration at this point, $\rho^* \cong 0.64 \text{ mg}_{\text{H}_2\text{O}}/\text{m}^2_{\text{[silica]}}$ would correspond to approximately 4.7 \AA^2 of the silica surface per water molecule (or $21 \text{ H}_2\text{O}/\text{nm}^2_{\text{[silica]}}$). This is about half of what is usually accepted for the water molecule span in bulk water and is obtained in numerical simulations of hydrogen-bonded water networks at idealized hydrophilic surfaces. For example, Argyris *et al.* simulated the behavior of a thin water film at a flat surface of crystalline silica with two alternative realistic extreme packings of silanol groups at the surface and found complete surface coverage by a hydrogen-bonded network at $\sim 10.6 \text{ H}_2\text{O}/\text{nm}^2_{\text{[substrate]}}$, either in the form of a dense monolayer or a layer that was sparsely arranged but twice as thick as the monolayer of water, depending on the silanol group concentration [55–59]. Additionally, Brovchenko, Oleinikova, and colleagues used somewhat different boundary conditions at the substrate surface—a uniform hydrophilic potential well at the surface—and obtained a similar value (about $11 \text{ H}_2\text{O}/\text{nm}^2_{\text{[substrate]}}$) [16,20,21]. The simulation results therefore suggest that about $11 \text{ H}_2\text{O}/\text{nm}^2_{\text{[substrate]}}$ are required for formation of the complete hydrogen-bonded network fully covering a perfect hydrophilic surface, with the structure of the water layer depending on the hydrophilic potential landscape at the substrate. This would give a percolation threshold when between one sixth and one third of the water molecules

disappear from the hydrogen-bonded network, depending on the substrate. For the dense single monolayer, the threshold is reached when approximately one third of the water molecules disappear from the hydrogen-bonded network [20]. For a sparse double-layer network, the threshold would already be reached when one third of the hydrogen-bonded water had vanished from the top layer, leaving behind 85% of the double-layer water, although this case has not yet been explored numerically.

Since formation of the threshold hydrogen-bonded network should not require the amounts of water observed in our experiment, the twofold difference must be associated with peculiarities of the fumed silica powders. Two factors may substantially influence the amount of water accumulated at the surface: heterogeneous organization of water molecules at the surface, and aggregation of primary silica particles and their further packing in powder. Surface imperfections impose formation of a heterogeneous structure of intermingled patches of differently structured water: weakly or strongly substrate-bonded spanning networks of hydrogen-bonded water, and patches where a lot of water molecules are not involved at all in the formation of the proton-conducting network [47]. Oleinikova *et al.* also found similar effects when simulating water behavior at protein surfaces, which are known to have properties of intermingled hydrophilic and hydrophobic regions surface properties [19]. As a result, there must be plenty of water present at the silica surface that does not take part in the formation of the proton-wire web.

On the other hand, there are mesoscopic effects augmenting the amount of moisture at the surface, associated with Aerosil primary particle aggregation in linear chains and further packing of the aggregates in bulk. When hydrating such rough systems, water has a tendency to instantly form pendular rings around points of contact between the primary particles, adding and storing a surplus of water in the system [60,61]. The amount of water accumulated in such places is substantial; it increases with increasing specific surface area (fineness of primary particles) [62], and these areas are the last to evacuate on dehydration, well after the percolation transition. In the same vein, Oleinikova *et al.* found numerically that loosening the packing (closeness) of the globular proteins has a strong influence on the observed threshold hydration; i.e., the looser the proteins, the higher the hydrogen-bonded network percolation threshold is [18]. Since while preparing samples we intentionally avoided compacting the powders and kept them as loose as possible to prevent gelation, this type of water accumulation in the samples would not be out of the question.

All in all, it is impossible to estimate quantitatively what fraction of water at the silica surface participates in protonic conduction, but there must be plenty of water in the silica powder that is not active in the conductivity percolation process. In this respect, the most rational of conductivity percolation models we mentioned above seems to be the “Swiss-cheese” model of Halperin *et al.* [50], with water film forming, on degradation, a system of channels, threads, links, blobs, pendular rings, and even nanodroplets—wetting or nonwetting, or both.

We note, finally, that conductivity percolation hydration thresholds [$h^* (\text{g}_{\text{H}_2\text{O}}/\text{g}_{\text{[substrate]}})$] for fumed silica and

biosystems vary dramatically from system to system even by two orders of magnitude (see Table 2 in [13]). This reflects differences in organization of water at the surfaces and also differences in the systems' mass, specific surfaces, geometry, and surface structure—both mechanical and chemical—so without detailed knowledge of these peculiarities, meaningful comparison is difficult. To account even partially for such specific details, Oleinikova *et al.* numerically studied the formation of spanning hydrogen-bonded water networks at surfaces of model globular protein powders, reasonably accounting for structure of the solvent-accessible surface (charged, polar, and nonpolar groups) and powder packing, to obtain percolation thresholds in agreement with the conductivity data [6,19].

V. CONCLUSIONS

This study followed the evolution of conductivity of dehydrating lightly wetted Aerosil fumed silica powders during natural dehydration to still air. At low levels of water content, we observed conductivity percolation and investigated conductivity scaling with hydration. We found that the scaling is typical for 2D or quasi-2D conducting systems, and is independent of the primary silica particle size. The scaling

exponent is close to unity, indicating the complex nature of the transition. Somewhat surprisingly, the percolation threshold appears when there is still plenty of water at the surface, i.e., corresponding roughly to twice the full hydration monolayer. This is far more than observed at the threshold in biological materials studied so far. The results are rationalized by taking into account the mechanical and chemical complexity of the surface and the “Swiss-cheese” structure of the receding water film. Last but not least, conductivity percolation on the wet surface of a hydrophilic inorganic solid was probably neither observed nor studied before.

ACKNOWLEDGMENTS

One of us (J.K.M.) expresses his gratitude to Ben Widom and David J. Schneider for insightful comments and discussions, and to Sarah Schneider for substantially improving the readability of the paper. The authors acknowledge the referees for useful comments; we modified the manuscript according to their comments and questions. We acknowledge the Polish Ministry of Science and Higher Education financial support under Grant No. NN202 105836, and the generous donation of Aerosil samples by Evonik Industries.

-
- [1] D. Stauffer and A. Aharony, *Introduction to Percolation Theory* (Taylor & Francis, Washington, DC, 1991).
- [2] F. Bruni, G. Careri, and A. C. Leopold, *Phys. Rev. A* **40**, 2803 (1989).
- [3] F. Bruni and A. C. Leopold, *Physiol. Plant.* **81**, 359 (1991).
- [4] J. A. Rupley, L. Siemianowski, G. Careri, and F. Bruni, *Proc. Natl. Acad. Sci. USA* **85**, 9022 (1988).
- [5] F. Bruni, G. Careri, and J. S. Clegg, *Biophys. J.* **55**, 331 (1989).
- [6] G. Careri, A. Giansanti, and J. Rupley, *Proc. Natl. Acad. Sci. USA* **83**, 6810 (1986).
- [7] G. Careri, A. Giansanti, and J. A. Rupley, *Phys. Rev. A* **37**, 2703 (1988).
- [8] G. Careri, M. Geraci, A. Giansanti, and J. A. Rupley, *Proc. Natl. Acad. Sci. USA* **82**, 5342 (1985).
- [9] M. Settles, W. Doster, F. Kremer, F. Post, and W. Schirmacher, *Philos. Mag. B* **65**, 861 (1992).
- [10] H. Haranczyk, M. Wnek, M. Olech, and J. K. Moscicki (in preparation).
- [11] H. Haranczyk, *On Water in Extremely Dry Biological Systems* (Jagiellonian University Press, Krakow, Poland, 2003).
- [12] D. Sokolowska, A. Krol-Otwinowska, and J. K. Moscicki, *Phys. Rev. E* **70**, 052901 (2004).
- [13] D. Sokolowska, A. Krol-Otwinowska, M. Bialecka, L. Fiedor, M. Szczygiel, and J. K. Moscicki, *J. Non-Cryst. Solids* **353**, 4541 (2007).
- [14] G. Careri and A. Giansanti, *Lett. Nuovo Cimento* **40**, 193 (1984).
- [15] P. R. C. Gaskoyne, R. Pethig, and A. Szent-Györgyi, *Proc. Natl. Acad. Sci. USA* **78**, 261 (1981).
- [16] P. Alpert, *Integr. Comp. Biol.* **45**, 685 (2005).
- [17] A. Oleinikova and I. Brovchenko, *Mol. Phys.* **104**, 3841 (2006).
- [18] I. Brovchenko and A. Oleinikova, *Chem. Phys. Chem.* **9**, 2695 (2008).
- [19] A. Oleinikova, N. Smolin, I. Brovchenko, A. Geiger, and R. Winter, *J. Phys. Chem. B* **109**, 1988 (2005).
- [20] N. Smolin, A. Oleinikova, I. Brovchenko, A. Geiger, and R. Winter, *J. Phys. Chem. B* **109**, 10995 (2005).
- [21] A. Oleinikova, I. Brovchenko, N. Smolin, A. Krukau, A. Geiger, and R. Winter, *Phys. Rev. Lett.* **95**, 247802 (2005).
- [22] A. Oleinikova, I. Brovchenko, and A. Geiger, *Physica A* **364**, 1 (2006).
- [23] I. Brovchenko, A. Krukau, N. Smolin, A. Oleinikova, A. Geiger, and R. Winter, *J. Chem. Phys.* **123**, 224905 (2005).
- [24] I. Brovchenko, A. Krukau, A. Oleinikova, and A. K. Mazur, *Phys. Rev. Lett.* **97**, 137801 (2006).
- [25] I. Brovchenko, A. Krukau, A. Oleinikova, and A. K. Mazur, *J. Phys. Chem. B* **111**, 3258 (2007).
- [26] A. Oleinikova, N. Smolin, and I. Brovchenko, *Biophys. J.* **93**, 2986 (2007).
- [27] I. Brovchenko, A. Krukau, A. Oleinikova, and A. K. Mazur, *J. Am. Chem. Soc.* **130**, 121 (2008).
- [28] R. P. Feynman, R. B. Leighton, and M. Sands, *Lectures on Physics*, Vol. 1 (Addison-Wesley, Reading, MA, 1964).
- [29] J. M. Normand, H. J. Herrmann, and M. Hajjar, *J. Stat. Phys.* **52**, 441 (1988).
- [30] *Monte Carlo Method in Condensed Matter Physics*, edited by K. Binder (Springer-Verlag, Berlin, 1992), p. 317.
- [31] V. V. Turov, V. M. Gun'ko, V. M. Bogatyrev, V. I. Zarko, S. P. Gorbik, E. M. Pakhlov, R. Leboda, O. V. Shulga, and A. A. Chuiko, *J. Colloid Interface Sci.* **283**, 329 (2005).
- [32] M. Nogami and Y. Abe, *Phys. Rev. B* **55**, 12108 (1997).
- [33] M. Nogami, *J. Sol-Gel Sci. Technol.* **31**, 359 (2004).
- [34] *Inorganic Materials for Catalyst Innovation: Aerosil, AEROX-IDE and SIPERNAT Metal Oxides and Silica Based Materials*, Industry Information 2242 (Evonik Degussa Co., Parsippany, NJ, 2010).

- [35] R. K. Iler, *Chemistry of Silica—Solubility, Polymerization, Colloid and Surface Properties and Biochemistry* (John Wiley & Sons, New York, 1979).
- [36] A. V. Volkov, A. V. Kiselev, and V. I. Lygin, *Zh. Fiz. Khim.* **48**, 1214 (1974) [*Russ. J. Phys. Chem.* **48**, 703 (1974)].
- [37] M. Ben-Chorin, F. Möller, F. Koch, W. Schirmacher, and M. Eberhard, *Phys. Rev. B* **51**, 2199 (1995).
- [38] A. Gutina, E. Axelrod, A. Puzenko, E. Rysiakiewicz-Pasek, N. Kozlovich, and Yu. Feldman, *J. Non-Cryst. Solids* **235–237**, 302 (1998).
- [39] E. Axelrod, A. Givant, J. Shappir, Yu. Feldman, and A. Sa'ar, *Phys. Rev. B* **65**, 165429 (2002).
- [40] P. Lunkenheimer and A. Loidl, *Phys. Rev. Lett.* **91**, 207601 (2003).
- [41] D. Hadži, *J. Mol. Struct.* **177**, 1 (1988).
- [42] V. V. Krasnogolovets, N. A. Protsenko, P. M. Tomchuk, and V. S. Guriev, *Int. J. Quantum Chem.* **23**, 327 (1988).
- [43] P. Pissis, J. Laudat, D. Daoukaki, and A. Kyritsis, *J. Non-Cryst. Solids* **171**, 201 (1994).
- [44] A. K. Jonscher, *Universal Relaxation Law* (Chelsea Dielectrics Press, London, 1996).
- [45] J. C. Rasaiah, S. Garde, and G. Hummer, *Annu. Rev. Phys. Chem.* **59**, 713 (2008).
- [46] J. Mathias and G. Wannemacher, *J. Colloid Interface Sci.* **125**, 61 (1988).
- [47] V. M. Gun'ko, V. V. Turov, V. M. Bogatyrev, V. I. Zarko, R. Leboda, E. V. Goncharuk, A. A. Novza, A. V. Turov, and A. A. Chuiko, *Adv. Colloid Interface Sci.* **18**, 125 (2005).
- [48] A. J. Page and R. P. Sear, *Phys. Rev. Lett.* **97**, 065701 (2006).
- [49] J. Hu, X.-D. Xiao, D. F. Ogletree, and M. Salmeron, *Science* **268**, 267 (1995).
- [50] B. I. Halperin, S. Feng, and P. N. Sen, *Phys. Rev. Lett.* **54**, 2391 (1985).
- [51] L. Benguigui, *Phys. Rev. B* **34**, 8176 (1986).
- [52] V. F. Petrenko and R. W. Whitworth, *Physics of Ice* (Oxford University Press, Oxford, UK, 1999), p. 97.
- [53] J. P. Straley, *Phys. Rev. B* **15**, 5733 (1977).
- [54] B. Berkowitz and R. Knight, *J. Stat. Phys.* **80**, 1415 (1995).
- [55] D. Argyris, N. R. Tummala, A. Striolo, and D. R. Cole, *J. Phys. Chem.* **112**, 13587 (2008).
- [56] C. G. Armistead, A. J. Tyler, F. H. Hambleton, S. A. Mitchell, and J. A. Hockey, *J. Phys. Chem.* **73**, 3947 (1969).
- [57] A. Burneau, B. Humbert, O. Barrès, J. P. Gallas, and J. C. Lavalley, *Adv. Chem. Ser.* **234**, 200 (1994).
- [58] E. F. Vansant, P. Van Der Voort, and K. C. Vrancken, *Characterization and Chemical Modification of the Silica Surface*, Studies in Surface Science and Catalysis, Vol. 93 (Elsevier, Amsterdam, 1995).
- [59] J. B. d'espinoze de la Caillerie, M. R. Aimeur, Y. E. Kortobi, and A. P. Legrand, *J. Colloid Interface Sci.* **194**, 434 (1997).
- [60] S. Bryant and A. Johnson, *J. Colloid Interface Sci.* **15**, 572 (2003).
- [61] H. Keskinen, S. Romakkaniemi, A. Jaatinen, P. Miettinen, E. Saukko, J. Jorma, J. M. Mäkelä, A. Virtanen, J. N. Smith, and A. Laaksonen, *Aerosol. Sci. Technol.* **45**, 1441 (2011).
- [62] V. M. Gun'ko, I. F. Mironyuk, V. I. Zarko, E. F. Voronin, V. V. Turov, E. M. Pakhlov, E. V. Goncharuk, Y. M. Nychiporuk, N. N. Vlasova, P. P. Gorbik, O. A. Mishchuk, A. A. Chuiko, Y. V. Kulik, B. B. Palyanytsya, S. V. Pakhovchishin, J. Skubiszewska-Zieba, W. Janusz, A. V. Turov, and R. Leboda, *J. Colloid Interface Sci.* **289**, 427 (2005).